

## MATERIALS SCIENCE

## Field-induced magnetic instability within a superconducting condensate

Daniel Gabriel Mazzone,<sup>1</sup> Stéphane Raymond,<sup>2\*</sup> Jorge Luis Gavilano,<sup>1</sup> Eric Ressouche,<sup>2</sup> Christof Niedermayer,<sup>1</sup> Jonas Okkels Birk,<sup>1,3</sup> Bachir Ouladdiaf,<sup>4</sup> Gaël Bastien,<sup>2</sup> Georg Knebel,<sup>2</sup> Dai Aoki,<sup>2</sup> Gérard Lapertot,<sup>2</sup> Michel Kenzelmann<sup>5\*</sup>

2017 © The Authors, some rights reserved; exclusive licensee American Association for the Advancement of Science. Distributed under a Creative Commons Attribution NonCommercial License 4.0 (CC BY-NC).

The application of magnetic fields, chemical substitution, or hydrostatic pressure to strongly correlated electron materials can stabilize electronic phases with different organizational principles. We present evidence for a field-induced quantum phase transition, in superconducting  $\text{Nd}_{0.05}\text{Ce}_{0.95}\text{CoIn}_5$ , that separates two antiferromagnetic phases with identical magnetic symmetry. At zero field, we find a spin-density wave that is suppressed at the critical field  $\mu_0 H^* = 8 \text{ T}$ . For  $H > H^*$ , a spin-density phase emerges and shares many properties with the Q phase in  $\text{CeCoIn}_5$ . These results suggest that the magnetic instability is not magnetically driven, and we propose that it is driven by a modification of superconducting condensate at  $H^*$ .

## INTRODUCTION

Although quantum mechanics was developed to treat nonrelativistic interacting particles, it has also been widely used to describe collective phenomena in condensed matter physics. A macroscopic quantity of interacting particles ( $\sim 10^{23}$ ) can give rise to novel quantum phases with emergent magnetic and transport properties that are currently hotly debated among theorists and experimentalists alike. Particularly exciting are quantum liquids, including superconducting condensates, that feature coherence phenomena over macroscopic length scales. Pressure, magnetic field, or chemical substitution can induce quantum phase transitions that originate from fluctuations that are governed by Heisenberg's uncertainty principle. These collective quantum fluctuations can trigger the collapse or emergence of an order parameter, and they can even dominate the finite temperature properties. Quantum fluctuations generally separate phases with different organizing principles (1, 2), leading to magnetic phases with different symmetry as the strength of the fluctuations evolve. This has been demonstrated, for instance, by quantum magnetic insulators (3).

Strong electronic correlations and quantum fluctuations are thought to be at the origin of unconventional superconductivity in many materials. Examples include the layered copper oxides (4), the iron-based pnictides, and the heavy-fermion (HF) superconductors (5).  $\text{CeCoIn}_5$  is an exceptional material because it features spin-density wave (SDW) order that emerges from the superconducting condensate (6). The material is an ultraclean, ambient-pressure,  $d_{x^2-y^2}$  superconductor ( $T_c = 2.3 \text{ K}$ ) (7) that displays a quasi-two-dimensional Fermi surface (8, 9). Superconductivity is Pauli-limited (10) and coexists at high fields with a SDW that emerges with an ordered moment  $\mu(11 \text{ T}) = 0.15(5)\mu_B$  (6, 11–14). Magnetism exists only inside the superconducting state and collapses in a first-order transition at the superconducting upper critical field. The ordering wave vector,  $\mathbf{Q} = (0.45, 0.45, 0.5)$ , is pinned along the nodes of the superconducting gap (11) and may result from the condensation of superconducting quasi-

particle excitations with increasing magnetic field (15, 16). All this provides evidence for a coupling between superconductivity and magnetic order (11, 12). However, the microscopic interpretation and the nature of the order parameters of this so-called Q phase are still debated (6, 15–23).

The Q phase is highly sensitive upon doping and has been suppressed in all previously reported cases (24–27). However, recent studies on  $\text{Nd}_{0.05}\text{Ce}_{0.95}\text{CoIn}_5$  (28, 29) revealed SDW magnetic order with a similar ordering wave vector as the Q phase for  $T < T_N = 0.8 \text{ K}$  at zero field (29). The family of Nd-substituted  $\text{CeCoIn}_5$ ,  $\text{Nd}_{1-x}\text{Ce}_x\text{CoIn}_5$ , displays a rich phase diagram featuring a HF ground state ( $x > 0.5$ ), superconductivity ( $x > 0.78$ ), and magnetism ( $x < 1$ ) (28). The substitution of Nd for Ce in  $\text{CeCoIn}_5$  introduces localized moments, reduces the hybridization of 4f-bands with the Fermi surface, and weakens the coherence of these heavy bands. This causes the destruction of itinerant magnetism and the emergence of localized moment magnetism at  $x < 0.5$ . Small Nd concentrations gradually weaken the superconducting pairing strength, as observed in the reduction in the specific-heat jump (28). The implantation of a small amount of Nd impurities in  $\text{CeCoIn}_5$  has a similar effect on superconductivity as the substitution with Kondo holes (29) and acts predominantly as random disorder (see the Supplementary Materials). However, the nature of the magnetic order for small Nd substitutions, such as in  $\text{Nd}_{0.05}\text{Ce}_{0.95}\text{CoIn}_5$ , and its relationship to the SDW in the Q phase is currently not understood.

## RESULTS

## Evidence for two distinct magnetic phases inside the superconducting condensate

We studied the magnetic order in  $\text{Nd}_{0.05}\text{Ce}_{0.95}\text{CoIn}_5$  as a function of field for  $\mathbf{H} \parallel [1 \bar{1} 0]$ . Figure 1 shows neutron diffraction data at several magnetic fields and  $T = 40 \text{ mK}$  along the  $(q, q, 0.5)$  reciprocal wave vector given in reciprocal lattice units. A well-defined magnetic Bragg peak is observed at zero field, consistent with previous measurements (29). With increasing field, the peak first increases in intensity but then completely vanishes around  $\mu_0 H^* \approx 8 \text{ T}$  (Fig. 1D). The key observation is that the peak reappears at higher fields, as shown in Fig. 1 (E and F). The magnetic Bragg peaks were fitted with a Gaussian line shape, showing that the width of the Bragg peaks is resolution-limited at all fields. The peak intensity,  $I_p$ , is shown in Fig. 2 as a function of field and provides direct evidence for two distinct magnetic phases: a low-field

<sup>1</sup>Laboratory for Neutron Scattering and Imaging, Paul Scherrer Institut, 5232 Villigen PSI, Switzerland. <sup>2</sup>Institute for Nanosciences and Cryogenics, Commissariat à l'Energie Atomique et aux Energies Alternatives, Université Grenoble Alpes, 38054 Grenoble, France. <sup>3</sup>Department of Physics, Technical University of Denmark (DTU), DK-2800 Kongens Lyngby, Denmark. <sup>4</sup>Institut Laue-Langevin, 38042 Grenoble, France. <sup>5</sup>Laboratory for Scientific Developments and Novel Materials, Paul Scherrer Institut, 5232 Villigen PSI, Switzerland.

\*Corresponding author. Email: michel.kenzelman@psi.ch (M.K.); raymond@ill.fr (S.R.)

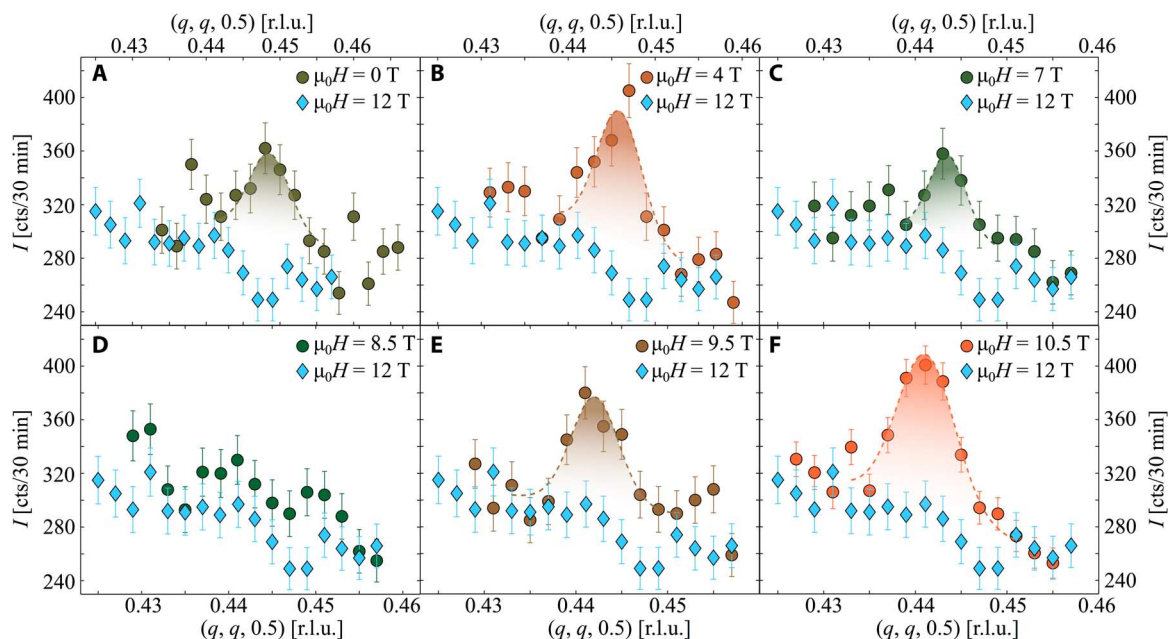


**Fig. 1. Magnetic order at various magnetic fields.** The scans display diffracted neutron intensity in counts per 30 minutes (cts/30 min) along the tetragonal plane  $(q, q, 0.5)$  in reciprocal lattice units (r.l.u.). The reflections correspond to magnetic Bragg peaks at  $\mu_0H = 0, 4, 7, 8.5, 9.5,$  and  $10.5$  T for (A) to (F), respectively. Background was measured at  $\mu_0H = 12$  T. All scans were taken at  $T = 40$  mK for  $\mathbf{H} \parallel [1 \bar{1} 0]$ . The integrated intensity grows for increasing fields up to 4 T, decreases for further field increments, and vanishes around  $\mu_0H^* \approx 8$  T. For higher fields, magnetic order reappears, increases in intensity, and collapses at  $\mu_0H = 11$  T.

phase (SDW phase) for  $\mu_0H < 8$  T and a high-field phase for  $8 \text{ T} < \mu_0H < 11$  T, which we call Q phase because it shares many properties with the Q phase of  $\text{CeCoIn}_5$ . The Q phase in  $\text{Nd}_{0.05}\text{Ce}_{0.95}\text{CoIn}_5$  appears for fields larger than 8 T, and its magnetic Bragg peak increases in intensity with increasing field. At  $\mu_0H = 11.0(2)$  T, it collapses in a sharp transition together with superconductivity. This shows that magnetic order is coupled to superconductivity at high fields—similar to the Q phase in undoped  $\text{CeCoIn}_5$ .

The  $HT$  phase diagram of the magnetic phases in  $\text{Nd}_{0.05}\text{Ce}_{0.95}\text{CoIn}_5$  is shown in Fig. 3 and shows additional similarities of the high-field phases in pure and doped  $\text{CeCoIn}_5$ : The Q phase in both compounds features very similar  $HT$  phase boundaries, and magnetic order is suppressed with increasing temperature. In a further similarity, the field-induced transition from the Q phase to the normal state in  $\text{Nd}_{0.05}\text{Ce}_{0.95}\text{CoIn}_5$  remains first-order at  $H_{c2}(T)$  for  $T < 300$  mK. Our results clearly establish that the Q phase in  $\text{CeCoIn}_5$  is stable under 5% Nd doping of the Ce site.

### Field-induced magnetic instability separates two SDWs with identical symmetry

As shown in Fig. 1D, a diffuse signal replaces the magnetic Bragg peak around  $\mu_0H^* \approx 8$  T. This demonstrates that there is a magnetic instability around  $H^*$  where magnetic order is absent and separates the SDW phase and the Q phase. Such diffuse scattering typically arises from short-range static or dynamic magnetic correlations. The field dependence of the magnetic Bragg peak intensity is linear as a function of field in the proximity of  $H^*$ , as shown in Fig. 2. Because the magnetic neutron intensity is proportional to the square of the magnetic moment, this means that the ordered magnetic moment  $M$  behaves as  $M = M_0|H/H^* - 1|^\beta$ , where  $\beta \approx 0.5$  and  $M_0 = 0.19(1)\mu_B$  for  $H < H^*$  and  $M_0 = 0.28(2)\mu_B$  for  $H > H^*$ , respectively with  $\mu_0H^* = 8.0(2)$  T. A mean-field exponent  $\beta = 0.5$  is also observed over a large field range as in the Q phase of the

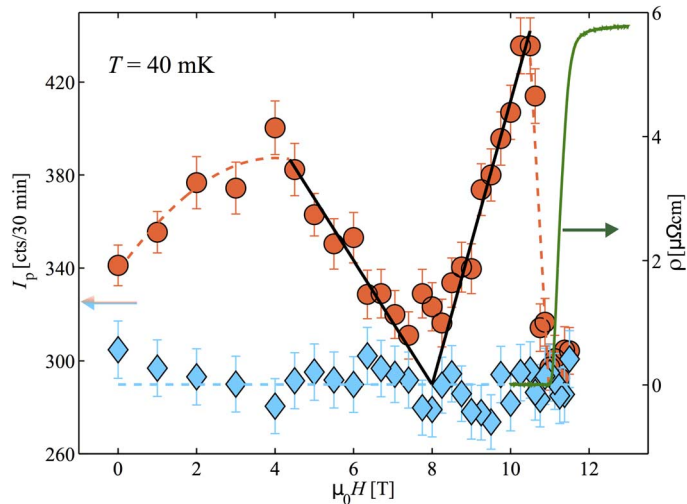


**Fig. 2. Discovery of a magnetic instability inside the superconducting phase.** The position-optimized peak intensity (red) shows two distinct magnetic phases inside the superconducting phase. Both phases vanish at  $\mu_0H^* = 8.0(2)$  T (solid and dashed lines are guides to the eye). Because of diffuse scattering, the magnetic intensity remains above the background level (blue) in the vicinity of  $H^*$ . The high-field phase collapses at the onset of the superconducting phase (resistivity along  $\mathbf{H} \parallel [1 \bar{1} 0]$  is shown in green),  $\mu_0H_{c2} = 11.0(2)$  T, providing evidence for a coupling between superconductivity and magnetic order.

undoped compound (6) and is expected for quantum phase transitions (30). Although we do not have direct evidence of quantum fluctuations, we point out that the  $HT$  phase diagram suggests the presence of a quantum critical region around  $H^*$  that expands with increasing temperature.

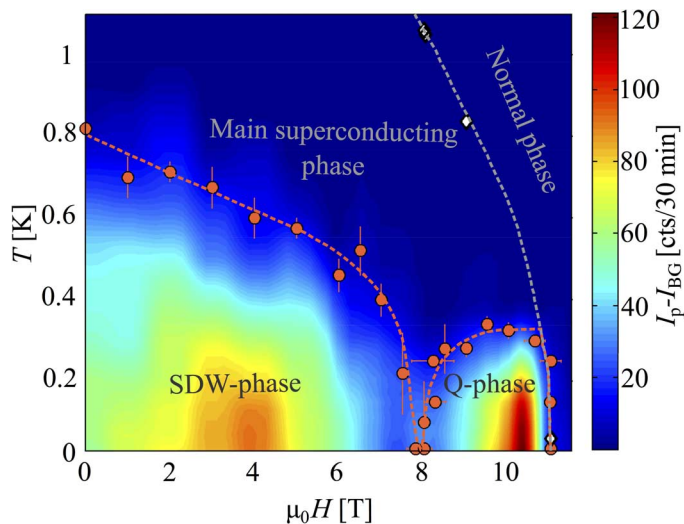


**Fig. 3. A magnetic instability separates two magnetic phases with identical symmetry inside the superconducting condensate.** *HT* phase diagram of  $\text{Nd}_{0.05}\text{Ce}_{0.95}\text{CoIn}_5$  for  $\mathbf{H} \parallel [1 \bar{1} 0]$ . The color scale represents the background-subtracted magnetic intensity. Orange circles display the magnetic phase boundaries obtained from neutron scattering results (orange dashed lines are guides to the eye). White diamonds show the superconducting phase boundary measured via electrical resistivity and heat capacity (the gray dashed line shows the superconducting phase boundary normalized from  $\text{CeCoIn}_5$ ). The color map reveals a field-induced instability at  $\mu_0 H^* = 8.0(2)$  T. The high-field phase, Q phase, increases linearly in intensity for increasing fields and collapses at the superconducting upper critical field  $\mu_0 H_{c2}$ .

The field dependence of the in-plane component of the wave vector transfer,  $q$ , is shown in Fig. 4. The data display a linear decrease in the wave number from  $q \approx 0.448$  at zero field to  $q \approx 0.441$  at 10.5 T and appear to be unaffected by the disappearance of magnetic order around  $\mu_0 H^* \approx 8$  T, which is probably related to robust features of the Fermi surface topology. The weak field dependence of the wave vector transfer is in contrast to the Q phase in  $\text{CeCoIn}_5$  where the wave vector is independent of the magnetic field (11, 12). The symmetry of the magnetic order is identical for the low-field SDW phase and high-field Q phase: At both zero field and  $\mu_0 H = 10.5$  T, an identical amplitude-modulated SDW with field-dependent magnetic moments aligned along the  $c$  axis (see Fig. 4, inset) and magnetic moments of  $\mu(0 \text{ T}) = 0.10(5)\mu_B$  and  $\mu(10.5 \text{ T}) = 0.15(5)\mu_B$  are found, respectively. For increasing fields, the magnetic peak intensity increases and reaches a broad maximum at  $\mu_0 H \approx 4$  T before it gradually weakens toward  $H^*$ . At  $\mu_0 H = 4$  T, the magnetic structure is also an amplitude-modulated SDW with a somewhat larger magnetic moment. This initial increase of intensity may result from a nonuniform magnetic domain population under a magnetic field. However, the magnetic structure determination clearly demonstrates that the symmetry of the magnetic structure does not change within the SDW phase.

## DISCUSSION

The identical magnetic symmetry of the ground states in the SDW phase and the Q phase demonstrates that the magnetic instability at  $\mu_0 H^* = 8$  T is not purely driven by magnetic fluctuations and that it must emerge from other types of fluctuations. Because the Kondo breakdown in  $\text{Nd}_{1-x}\text{Ce}_x\text{CoIn}_5$  occurs around  $x = 0.5$  (28), we exclude the possibility that the observed magnetic instability for  $x = 0.95$  is driven by charge valence fluctuations. On the other hand, it is well known

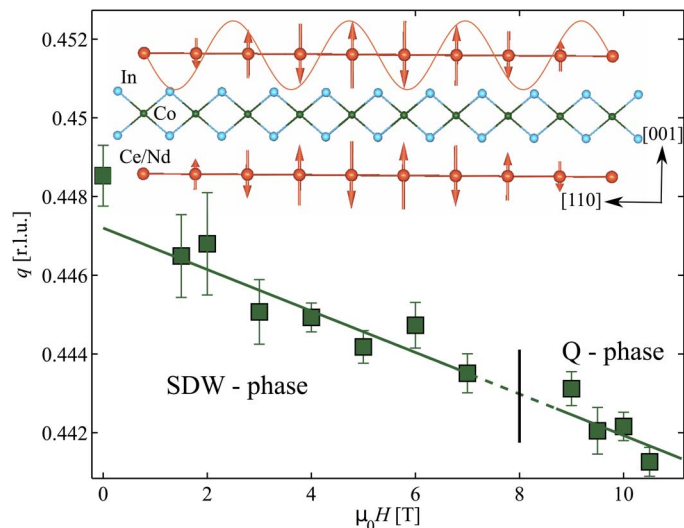


**Fig. 4. Field-dependent wave vector and magnetic structure.** The in-plane component of the propagation vector decreases linearly with increasing fields. Inset: Magnetic structure refined at  $\mu_0 H = 0$  and 10.5 T. An amplitude-modulated structure with a moment configuration perpendicular to the basal plane is found, similar to the Q phase of  $\text{CeCoIn}_5$ .

that Pauli-limited superconductors feature instabilities toward complex superconducting phases at high fields, including modulated superconductivity and phases of coexisting magnetic and superconducting order (20, 31, 32). Our results may be explained by a modification of the superconducting condensate that induces a change in the magnetic properties. This is consistent with a recently proposed scenario in undoped  $\text{CeCoIn}_5$ , where SDW order only exists for fields higher than  $\mu_0 H = 9.8$  T and is induced by the emergence of p-wave superconductivity in the d-wave condensate (6, 12, 33, 34). The scenario of novel superconductivity for high fields in the tetragonal plane of  $\text{CeCoIn}_5$  is expected from a number of microscopic theories (16–22). We note that the *HT* phase diagram of  $\text{Nd}_{0.05}\text{Ce}_{0.95}\text{CoIn}_5$  shows some qualitative similarities with the *xT* phase diagram of La-based cuprate  $\text{La}_{2-x}\text{Ba}_x\text{CuO}_4$ , where two superconducting phases exist in the presence of charge and stripe order and are separated by one or more critical points (35). For  $\text{Nd}_{0.05}\text{Ce}_{0.95}\text{CoIn}_5$ , it needs to be determined whether the magnetic instability is caused by a single or several quantum phase transitions. In this respect, it will be important to study the *HT* phase diagrams of  $\text{Nd}_{1-x}\text{Ce}_x\text{CoIn}_5$  for  $x > 0.95$ .

In summary, we report the discovery of a magnetic instability region inside the superconducting phase of  $\text{Nd}_{0.05}\text{Ce}_{0.95}\text{CoIn}_5$  that separates two antiferromagnetic phases with identical symmetry. Whereas a low-field SDW is suppressed at  $\mu_0 H^* = 8$  T, another SDW emerges from fields  $\mu_0 H^* > 8$  T and shares many properties with the Q phase of  $\text{CeCoIn}_5$ , such as the sudden collapse of the SDW at the upper critical field. Our experiment shows that the Q phase in  $\text{CeCoIn}_5$  is stable under 5% Nd doping of the Ce site. The identical magnetic symmetry of the two magnetically ordered phases suggests a quantum phase transition driven by a modification of the superconducting condensate.

## MATERIAL AND METHODS

Neutron diffraction measurements were carried out on the thermal-neutron lifting-counter two-axis spectrometer D23, the single-crystal four-circle diffractometer D10, the cold-neutron three-axis spectrometer

IN12 at the Institut Laue-Langevin (Grenoble, France), and the cold-neutron triple-axis spectrometer RITA-II at the Swiss Spallation Neutron Source SINQ, Paul Scherrer Institut (Villigen, Switzerland). For all measurements, the same single crystal of mass  $m = 64$  mg was used (see also the Supplementary Materials). The experiments required temperatures down to  $T = 40$  mK and maximal fields of  $\mu_0 H = 12$  T, which were achieved using vertical-field magnets with dilution inserts. On D23, an incident neutron wavelength  $\lambda = 1.28$  Å was used. The experiment on D10 was conducted with a neutron wavelength  $\lambda = 2.36$  Å. For the experiment, we used the  $^3\text{He}$  single detector in a four-circle setup and optimized the signal-to-noise ratio via the analyzer option of the instrument. A clean wavelength  $\lambda = 4.83$  Å was derived from a velocity selector and double-focusing pyrolytic graphite monochromator on IN12. The neutrons were collimated by  $\alpha = 80'$  before scattering at the sample. On RITA-II, we used a wavelength  $\lambda = 4.217$  Å. The high-energy background was minimized with a collimator ( $\alpha = 80'$ ), followed by a pyrolytic graphite filter before and a beryllium filter after the sample. The signal was recorded from the central analyzer blade of the RITA-II nine-bladed multianalyzer, and the background in Fig. 2 was obtained from the two neighboring blades.

The magnetic structure at zero field was obtained from the data measured on D10. Six independent magnetic Bragg reflections were analyzed using the three possible irreducible representations. The amplitude-modulated SDW along the  $c$  axis with  $\mu(0\text{ T}) = 0.10(5)\mu_B$  results in  $R_f = 13.6\%$ . Refinements in other representations yield  $R_f > 43\%$  constantly. For the magnetic structure analysis at  $\mu_0 H = 10.5$  T at RITA-II, six independent reflections were used. For the best refinement, in the amplitude-modulated representation with  $\mu(0\text{ T}) = 0.15(5)\mu_B$ ,  $R_f$  equals 12.6%, whereas models in other representations yield  $R_f > 30\%$ . In each model, equally populated domains,  $\mathbf{q} = (q, \pm q, 0.5)$ , were assumed, and the inset of Fig. 4 shows one of the two domains. For the refinements, the FullProf suite was used (36). The prefactors  $M_0$  above and below the  $H^*$  were obtained by a fit of the field-dependent ordered magnetic moment. This field dependence was recovered from refinements of the integrated intensity in the amplitude-modulated representation that were calculated from the peak intensities shown in Fig. 2. The superconducting upper critical field,  $H_{c2}(T)$ , was measured by means of electrical resistivity and heat capacity at Commissariat à l'Énergie Atomique et aux Énergies Alternatives in Grenoble, France. These experiments were performed on a small part of the single crystal used for neutron diffraction and on small crystals of the same batch. Experimental data are shown in the Supplementary Materials.

The magnetic phase diagram in Fig. 3 was realized via neutron diffraction data measured at the peak-optimized position of the magnetic Bragg peak on the instruments RITA-II and IN12. The phase boundary was obtained from temperature scans at  $\mu_0 H = 1, 2, 3, 4, 4.5, 5, 5.5, 6, 6.5, 7, 7.5, 8, 8.5, 9, 9.5,$  and 10 T, as well as field scans at  $T = 40, 150, 250,$  and 300 mK. The field scan at  $T = 40$  mK is shown in Fig. 2, and the temperature scans at  $\mu_0 H = 7$  to 9.5 T are displayed in the Supplementary Materials. The color plot represents the monitor-normalized background-subtracted peak intensity. Points among the measured data points were interpolated from the nearest neighbor-measured peak intensities.

## SUPPLEMENTARY MATERIALS

Supplementary material for this article is available at <http://advances.sciencemag.org/cgi/content/full/3/5/e1602055/DC1>

Supplementary Materials and Methods  
fig. S1. Macroscopic results.

fig. S2. Temperature dependence of magnetic intensity in the critical region.

Reference (37)

## REFERENCES AND NOTES

1. P. Gegenwart, S. Qimiao, F. Steglich, Quantum criticality in heavy-fermion metals. *Nat. Phys.* **4**, 186–197 (2008).
2. S. Qimiao, F. Steglich, Heavy fermions and quantum phase transitions. *Science* **329**, 1161–1166 (2010).
3. V. Zapf, M. Jaime, C. D. Batista, Bose-Einstein condensation in quantum magnets. *Rev. Mod. Phys.* **86**, 563–614 (2014).
4. N. Doiron-Leyraud, C. Proust, D. LeBoeuf, J. Levallois, J.-B. Bonnemaison, R. Liang, D. A. Bonn, W. N. Hardy, L. Taillefer, Quantum oscillations and the Fermi surface in an underdoped high- $T_c$  superconductor. *Nature* **447**, 565–568 (2007).
5. N. D. Mathur, F. M. Grosche, S. R. Julian, I. R. Walker, D. M. Freye, R. K. W. Haselwimmer, G. G. Lonzarich, Magnetically mediated superconductivity in heavy fermion compounds. *Nature* **394**, 39–43 (1998).
6. S. Gerber, M. Bartkowiak, J. L. Gavilano, E. Ressouche, N. Egetenmeyer, C. Niedermayer, A. D. Bianchi, R. Movshovich, E. D. Bauer, J. D. Thompson, M. Kenzelmann, Switching of magnetic domains reveals evidence for spatially inhomogeneous superconductivity. *Nat. Phys.* **10**, 126–129 (2014).
7. C. Petrovic, P. G. Pagliuso, M. F. Hundley, R. Movshovich, J. L. Sarrao, J. D. Thompson, Z. Fisk, P. Monthoux, Heavy-fermion superconductivity in  $\text{CeCoIn}_5$  at 2.3 K. *J. Phys. Condens. Matter* **13**, L337–L342 (2001).
8. R. Settai, H. Shishido, S. Ikeda, Y. Murakawa, M. Nakashima, D. Aoki, Y. Haga, H. Harima, Y. Onuki, Quasi-two-dimensional Fermi surfaces and the de Haas-van Alphen oscillation in both the normal and the superconducting mixed states of  $\text{CeCoIn}_5$ . *J. Phys. Condens. Matter* **13**, L627–L634 (2001).
9. D. Hall, E. C. Palm, T. P. Murphy, S. W. Tozer, Z. Fisk, U. Alver, R. G. Goodrich, J. L. Sarrao, P. G. Pagliuso, T. Ebihara, Fermi surface of the heavy-fermion superconductor  $\text{CeCoIn}_5$ : The de Haas-van Alphen effect in the normal state. *Phys. Rev. B* **64**, 212508 (2001).
10. A. Bianchi, R. Movshovich, C. Capan, P. G. Pagliuso, J. L. Sarrao, Possible Fulde-Ferrell-Larkin-Ovchinnikov superconducting state in  $\text{CeCoIn}_5$ . *Phys. Rev. Lett.* **91**, 187004 (2003).
11. M. Kenzelmann, T. Strässle, C. Niedermayer, M. Sigrüst, B. Padmanabhan, M. Zolliker, A. D. Bianchi, R. Movshovich, E. D. Bauer, J. L. Sarrao, J. D. Thompson, Coupled superconducting and magnetic order in  $\text{CeCoIn}_5$ . *Science* **321**, 1652–1654 (2008).
12. M. Kenzelmann, S. Gerber, N. Egetenmeyer, L. L. Gavilano, Th. Strässle, A. D. Bianchi, E. Ressouche, R. Movshovich, E. D. Bauer, J. L. Sarrao, J. D. Thompson, Evidence for magnetically driven superconducting Q phase of  $\text{CeCoIn}_5$ . *Phys. Rev. Lett.* **104**, 127001 (2010).
13. B.-L. Young, R. R. Urbano, N. J. Curro, J. D. Thompson, J. L. Sarrao, A. B. Vorontsov, M. J. Graf, Microscopic evidence for field-induced magnetism in  $\text{CeCoIn}_5$ . *Phys. Rev. Lett.* **98**, 03640 (2007).
14. G. Koutroulakis, M. D. Stewart Jr., V. F. Mitrović, M. Horvatić, C. Berthier, G. Lapertot, J. Flouquet, Field evolution of coexisting superconducting and magnetic orders in  $\text{CeCoIn}_5$ . *Phys. Rev. Lett.* **104**, 087001 (2010).
15. S. Raymond, G. Lapertot, Ising incommensurate spin resonance of  $\text{CeCoIn}_5$ : A dynamic precursor of the Q phase. *Phys. Rev. Lett.* **115**, 037001 (2015).
16. V. P. Michal, V. P. Mineev, Field-induced spin-exciton condensation in the  $d_{x^2-y^2}$ -wave superconducting  $\text{CeCoIn}_5$ . *Phys. Rev. B* **84**, 052508 (2011).
17. Y. Yanase, M. Sigrüst, Antiferromagnetic order and  $\pi$ -triplet pairing in the Fulde-Ferrell-Larkin-Ovchinnikov state. *J. Phys. Soc. Jpn.* **78**, 114715 (2009).
18. Y. Hatakeyama, R. Ikeda, Antiferromagnetic order oriented by Fulde-Ferrell-Larkin-Ovchinnikov superconducting order. *Phys. Rev. B* **91**, 094504 (2015).
19. Y. Kato, C. D. Batista, I. Vekhter, Antiferromagnetic order in Pauli-limited unconventional superconductors. *Phys. Rev. Lett.* **107**, 096401 (2011).
20. K. M. Suzuki, M. Ichioka, K. Machida, Theory of an inherent spin-density-wave instability due to vortices in superconductors with strong Pauli effects. *Phys. Rev. B* **83**, 140503 (2011).
21. A. Aperis, G. Varelogiannis, P. B. Littlewood, Magnetic-field-induced pattern of coexisting condensates in the superconducting state of  $\text{CeCoIn}_5$ . *Phys. Rev. Lett.* **104**, 216403 (2010).
22. Y. Matsuda, H. Shimahara, Fulde-Ferrell-Larkin-Ovchinnikov state in heavy Fermion superconductors. *J. Phys. Soc. Jpn.* **76**, 051005 (2007).
23. K. Kumagai, H. Shishido, T. Shibauchi, Y. Matsuda, Evolution of paramagnetic quasiparticle excitations emerged in the high-field superconducting phase of  $\text{CeCoIn}_5$ . *Phys. Rev. Lett.* **106**, 137004 (2011).
24. S. Seo, X. Lu, J.-X. Zhu, R. R. Urbano, N. Curro, E. D. Bauer, V. A. Sidorov, L. D. Pham, T. Park, Z. Fisk, J. D. Thompson, Disorder in quantum critical superconductors. *Nat. Phys.* **10**, 120–125 (2014).
25. S. M. Ramos, M. B. Fontes, E. N. Hering, M. A. Continentino, E. Baggio-Saitovich, F. D. Neto, E. M. Bittar, P. G. Pagliuso, E. D. Bauer, J. L. Sarrao, J. D. Thompson, Superconducting quantum critical point in  $\text{CeCoIn}_{5-x}\text{Sn}_x$ . *Phys. Rev. Lett.* **105**, 126401 (2010).
26. L. D. Pham, T. Park, S. Maquilon, J. D. Thompson, Z. Fisk, Reversible tuning of the heavy-fermion ground state in  $\text{CeCoIn}_5$ . *Phys. Rev. Lett.* **97**, 056404 (2006).
27. C. H. Booth, E. D. Bauer, A. D. Bianchi, F. Ronning, J. D. Thompson, J. L. Sarrao, J. Y. Cho, J. Y. Chan, C. Capan, Z. Fisk, Local structure and site occupancy of Cd and Hg substitutions in  $\text{CeTIn}_5$  ( $T = \text{Co, Rh and Ir}$ ). *Phys. Rev. B* **79**, 144519 (2009).

28. R. Hu, Y. Lee, J. Hudis, V. F. Mitrovic, C. Petrovic, Composition and field-tuned magnetism and superconductivity in  $\text{Nd}_{1-x}\text{Ce}_x\text{CoIn}_5$ . *Phys. Rev. B* **77**, 165129 (2008).
29. S. Raymond, S. M. Ramos, D. Aoki, G. Knebel, V. P. Mineev, G. Lapertot, Magnetic order in  $\text{Ce}_{0.95}\text{Nd}_{0.05}\text{CoIn}_5$ : The Q-phase at zero magnetic field. *J. Phys. Soc. Jpn.* **83**, 013707 (2014).
30. J. A. Hertz, Quantum critical phenomena. *Phys. Rev. B* **14**, 1165–1184 (1976).
31. K. Yang, S. L. Sondhi, Response of  $d_{x^2-y^2}$  superconductor to Zeeman magnetic field. *Phys. Rev. B* **57**, 8566–8570 (1998).
32. M. Kenzelmann, Exotic magnetic states in Pauli-limited superconductors. *Rep. Prog. Phys.* **80**, 034501 (2017).
33. D. Y. Kim, S.-Z. Lin, F. Weickert, M. Kenzelmann, E. D. Bauer, F. Ronning, J. D. Thompson, R. Movshovich, Intertwined orders in heavy-fermion superconductor  $\text{CeCoIn}_5$ . *Phys. Rev. X* **6**, 041059 (2016).
34. D. F. Agterberg, M. Sigrist, H. Tsunetsugu, Order parameter and vortices in the superconducting Q phase of  $\text{CeCoIn}_5$ . *Phys. Rev. Lett.* **102**, 207004 (2009).
35. M. Hückler, M. v. Zimmermann, G. D. Gu, Z. J. Xu, J. S. Wenn, G. Xu, H. J. Kang, A. Zheludev, J. M. Tranquada, Stripe order in superconducting  $\text{La}_{2-x}\text{Ba}_x\text{CuO}_4$  ( $0.095 \leq x \leq 0.155$ ). *Phys. Rev. B* **83**, 104506 (2011).
36. J. Rodríguez-Carvajal, Recent advances in magnetic structure determination by neutron powder diffraction. *Phys. B* **192**, 55–69 (1993).
37. L. Howald, G. Seyfarth, G. Knebel, D. Aoki, G. Lapertot, D. Aoki, J.-P. Brison, Behavior of the quantum critical point and the Fermi-liquid domain in the heavy fermion superconductor  $\text{CeCoIn}_5$  studied by resistivity. *J. Phys. Soc. Jpn.* **80**, 024710 (2011).

**Acknowledgments:** We acknowledge the Institut Laue-Langevin and the Paul Scherrer Institut for the allocated beam time on D23, D10, IN12, and RITA-II. We thank P. Fouilloux, P. Decarpenrie, B. Vettard, K. Mony, X. Tonon, B. Grenier, M. Zolliker, and M. Bartkowiak

for technical assistance. Discussions with M. Sigrist and S. Gerber are acknowledged. **Funding:** We thank the Swiss National Science Foundation (grant nos. 200021\_147071 and 200021\_138018). This work was additionally supported by the Swiss State Secretariat for Education, Research, and Innovation through a Collaboration Research Group grant. The research also received funding from the European Community's Seventh Framework Programme (FP7/2007-2013) under grant agreement no. 290605 (PSI-FELLOW/COFUND). We also acknowledge the Danish neutron society community Danscatt. **Author contributions:** D.G.M., S.R., J.L.G., and M.K. planned and led the project. The neutron experiments were performed by D.G.M., S.R., J.L.G., E.R., C.N., J.O.B., B.O., and M.K. The resistivity and heat capacity measurements were performed by G.B., G.K., and D.A. The sample was grown by G.L., and the data were analyzed by D.G.M. The manuscript was written by D.G.M., S.R., J.L.G., and M.K. with the input of all coauthors. **Competing interests:** All authors declare that they have no competing interests. **Data and materials availability:** All data needed to evaluate the conclusions in the paper are present in the paper and/or the Supplementary Materials. Additional data related to this paper may be requested from the authors. Correspondence and requests for materials should be addressed either to M.K. or to S.R. (emails: michel.kenzelmann@psi.ch and raymond@ill.fr).

Submitted 29 August 2016

Accepted 20 March 2017

Published 19 May 2017

10.1126/sciadv.1602055

**Citation:** D. G. Mazzone, S. Raymond, J. L. Gavilano, E. Ressouche, C. Niedermayer, J. O. Birk, B. Ouladdiaf, G. Bastien, G. Knebel, D. Aoki, G. Lapertot, M. Kenzelmann, Field-induced magnetic instability within a superconducting condensate. *Sci. Adv.* **3**, e1602055 (2017).

## Field-induced magnetic instability within a superconducting condensate

Daniel Gabriel Mazzone, Stéphane Raymond, Jorge Luis Gavilano, Eric Ressouche, Christof Niedermayer, Jonas Okkels Birk, Bachir Ouladdiaf, Gaël Bastien, Georg Knebel, Dai Aoki, Gérard Lapertot and Michel Kenzelmann

*Sci Adv* 3 (5), e1602055.  
DOI: 10.1126/sciadv.1602055

### ARTICLE TOOLS

<http://advances.sciencemag.org/content/3/5/e1602055>

### SUPPLEMENTARY MATERIALS

<http://advances.sciencemag.org/content/suppl/2017/05/15/3.5.e1602055.DC1>

### REFERENCES

This article cites 37 articles, 2 of which you can access for free  
<http://advances.sciencemag.org/content/3/5/e1602055#BIBL>

### PERMISSIONS

<http://www.sciencemag.org/help/reprints-and-permissions>

Use of this article is subject to the [Terms of Service](#)

---

*Science Advances* (ISSN 2375-2548) is published by the American Association for the Advancement of Science, 1200 New York Avenue NW, Washington, DC 20005. The title *Science Advances* is a registered trademark of AAAS.

Copyright © 2017, The Authors